Three-dimensional measurement endoscope system with virtual rulers

Hiromasa Nakatani
Shizuoka University
Computer Science Department
Hamamatsu, Shizuoka 432-8011
Japan

Keiichi Abe
Aichi Institute of Technology
Applied Information Sciences
Yachigusa 1247
Toyota, Aichi 470-0392
Japan

Atsuo Miyakawa
Susumu Terakawa
Hamamatsu University School of Medicine
Photon Medical Research Center
Hamamatsu, Shizuoka 431-3192
Japan

Abstract. Conventional endoscopic images do not provide quantitative 3-D information. We present an endoscope system that can measure the size and position of an object in real time. Our endoscope contains four laser beam sources and a camera. The procedural steps for 3-D measurements are as follows. First, to obtain the function that maps 2-D coordinates of an image point to its 3-D coordinates in 3-D space, we observe a standard chart with the endoscope lens and determine the correspondence between the image and object height. In addition to the mapping, this function can correct barrel-shaped distortion of endoscopic images. The system detects laser spots on an object surface automatically using a template matching method, and maps the 2-D coordinates of the laser spots to the 3-D coordinates by the triangulation method. Then the system calculates the magnification ratio on the object plane, which is perpendicular to the optical axis and passes the laser spot, so that the system can superimpose a ruler whose scale fits the 3-D coordinates of the object. Thus, physicians can measure the size and position of objects in real time on undistorted images similar to placing rulers on the surface of an organ.
 [DOI: 10.1117/1.2800758]

Keywords: 3-D measurement; endoscope; virtual ruler; imaging; barrel distortion; laser.

Paper 07013SSR received Jan. 15, 2007; revised manuscript received May 25, 2007; accepted for publication Jun. 4, 2007; published online Nov. 5, 2007.

1 Introduction

Endoscopy has been widely used as a minimally invasive diagnostic medical procedure.[1,2] Conventional endoscopes with a wide-angle lens can provide physicians with a wide view in the long distance and a magnified view in the short distance. However, since the appearance of an object changes by its distance from the lens, the exact size or location is not obvious only from an endoscopic image. When physicians are required to measure or record the size of the object, they have to thrust a small ruler through a forceps channel in the endoscope and take an internal picture while keeping the ruler within view. This procedure, however, is time consuming even for an experienced endoscopist, and the resulting data may lack precision. Since they can only obtain a rough approximation of the distance, it is difficult for them to judge, for example, whether the size of a tumor is increasing or decreasing. Thus, those methods that can produce an objective 3-D measurement have long been expected.

Recently, novel technologies such as virtual reality and augmented reality are applied to endoscopy and produce 3-D or stereoscopic images using 3-D data from MRI or CT scans.[3–5] Regular endoscopes, however, still play a main role in visual inspection and minimally invasive surgery, and 3-D display or measurement that uses only endoscopes is also widely studied. For example, a binocular stereoscopic approach is proposed for increasing the depth and spatial perception of a monocular video endoscope.[6] 3-D images are also obtained by analyzing the reflection of multicolored light that is projected onto tissue.[7] There have been proposals to project a laser beam to generate a grid on an object and measure the three dimensions by tracing manually the outline of an object and beam spots,[8] or to project a striped pattern of light for the 3-D measurements on the stripes.[9] In this work, we propose an endoscope system that projects multiple laser beams, detects the laser spots automatically, and can display rulers on the endoscopic images, so that physicians can measure the size and position of an object in real time.

2 Methods for Three-Dimensional Measurement

2.1 *System Outline*

Our endoscope contains four laser beams, which are directed via optical fibers and set parallel to the optical axis of the camera (Fig. 1). The laser beams are projected from the tip of the endoscope onto an object under inspection, and their spots are automatically detected by image processing techniques. Using the 2-D coordinates of those spots, we can calculate the corresponding 3-D coordinate by the triangulation, and can display virtual rulers on the endoscope monitor. At the same time, we can correct barrel distortion associated by the wide angle lens of the endoscope. The procedural steps are as follows.

Address all correspondence to Hiromasa Nakatani, Shizuoka University, Computer Science Department, Hamamatsu, Shizuoka 432-8011, Japan. Tel: 81 53 478 1482; Fax: 81 53 478 1482; E-mail: nakatani@inf.shizuoka.ac.jp

1083-3668/2007/12(5)/051803/6/$25.00 © 2007 SPIE

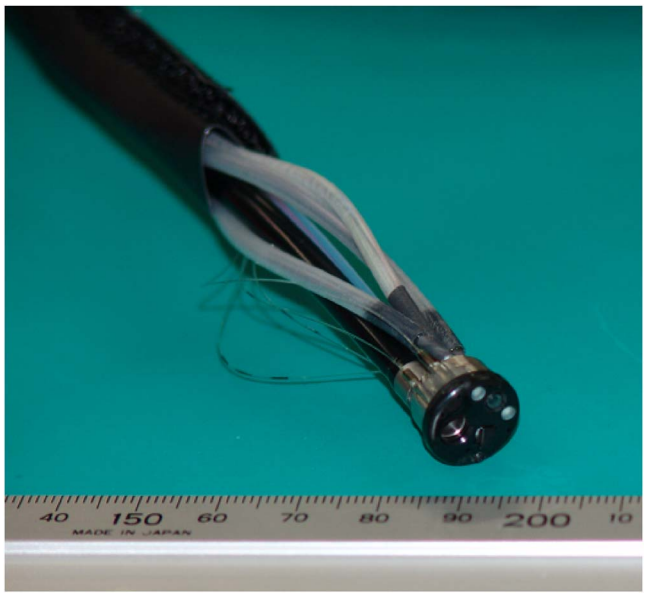

Fig. 1 Distal end of the laser endoscope.

2.2 *Barrel Distortion Correction*

The wide-angle lenses used in regular endoscopes are susceptible to barrel distortions, which can disturb the physicians' visual perception of shape and size of lesions or suspicious regions.

To remove the distortion from observed images we have to relate the distance of a pixel from the optical axis in an observed image to the corresponding distance in an undistorted image. Once the distortion function is determined, we can use it for all the source images, since the distortion function that gives the correspondences is unique to the particular lens. We observe a test chart shown in Fig. 2(a) with the endoscope and determine the distortion function by measuring the distances of several points on the distorted image and those on the test chart. Figure 3 shows the resulting distortion function, Fig. 2(a) shows the source image, and 2(b) the corrected image.

2.3 *Laser Spot Detection*

To measure the 3-D coordinates of laser spots, the system locates those points in an image using a template matching method.[10] Since the physical configurations of the camera and the laser beams are *a priori* given, the search areas for the laser spots are limited, and it is not necessary to search the whole image. Since the laser beams of our system are set to

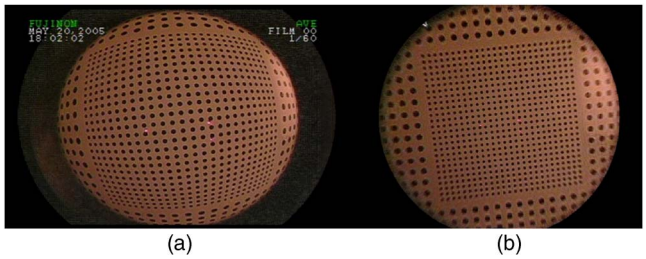

Fig. 2 Barrel distortion correction (a) distorted and (b) corrected image.

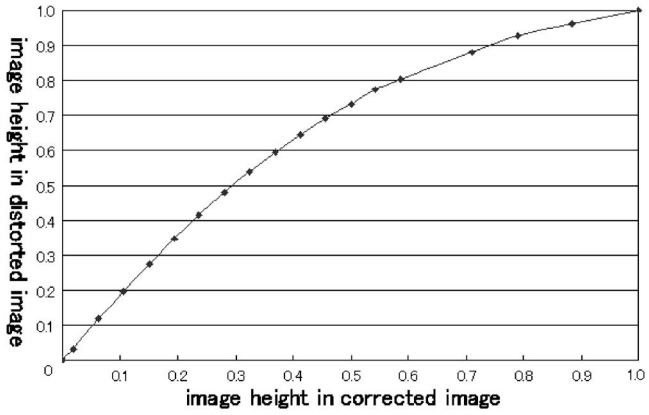

Fig. 3 Distortion function.

be parallel to the optical axis of the camera lens, the search area for the leaser spots are restricted on those lines that are depicted as white lines in Fig. 4.

To determine the location of the laser spots, we compare the density values of each pixel, which are transformed from 8-bit RGB values. To judge the similarity to the laser spot, we measure the density distribution and its deviation in the neighborhood of each pixel. Those pixels that have maximum similarity and larger deviation than a predetermined threshold are identified as the laser spots. The similarity is defined by the correlation between an input image and a Gaussian distribution, since we regard the density profile of the laser spot as Gaussian.

As is shown in our experiments, endoscopic images may have reflection highlights. To prevent the highlights from disturbing the laser spot detection, we regard such pixels that have high values of G or B elements of RGB as highlights and neglect them from the laser spot detection.

2.4 *Calculation of Three-Dimensional Coordinates*

Figure 5 illustrates the calculation of the 3-D coordinates of the laser spots. Let the lens optical center O be the origin of the 3-D space, the camera optical axis be the z axis, $L(X_L, Y_L, Z_L)$ denote the laser beam source, $P(X_p, Y_p, Z_p)$ denote the laser spot on an object, and $p(x_p, y_p, f)$ denote the

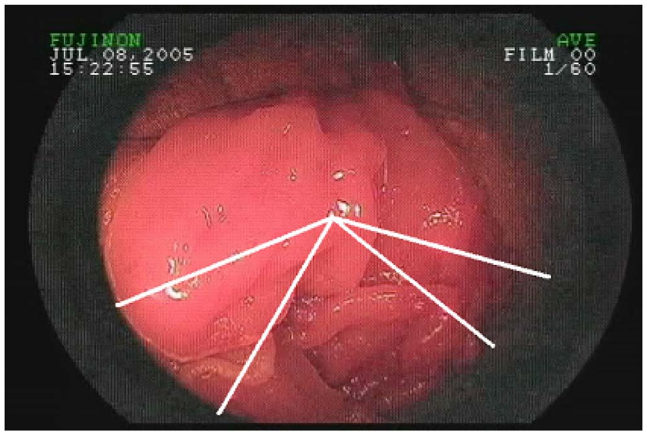

Fig. 4 Search area for laser spots.

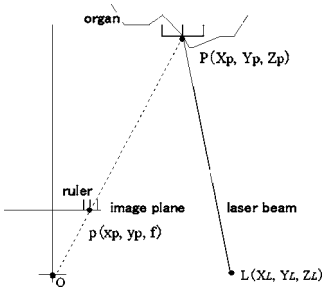

Fig. 5 Laser spot and ruler.

laser spot projected on the image plan, where f is the focal length of the lens. Here, for ease of explanation, the image plane is drawn in-between the lens and the object, though it actually is located on the opposite side of the object from the lens.

The 2-D coordinates (x_p, y_p) of the projection on the image plane of the laser spot (X_p, Y_p, Z_p) can be calculated after the spot is detected by the method mentioned in Sec. 2.3. Here, the line connecting the origin O and the laser spot $P(X_p, Y_p, Z_p)$ is given by

$$\frac{x}{x_p} = \frac{y}{y_p} = \frac{z}{f}, \tag{1}$$

and the line connecting the laser beam source $L(X_L, Y_L, Z_L)$ and the laser spot $P(X_p, Y_p, Z_p)$ is given by

$$\frac{x - X_L}{B_X} = \frac{y - Y_L}{B_Y} = \frac{z - Z_L}{B_Z}, \tag{2}$$

where (B_X, B_Y, B_Z) is the direction vector of the laser beam, which is determined when the system is designed. Even if we do not know the value of the direction vector, we can obtain it empirically by measuring the beam spot on a screen that is set at a known distance. In this case, the direction vector can be determined from the position of the spot (X_s, Y_s, Z_s):

$$(B_X, B_Y, B_Z) = (X_s - X_L, Y_s - Y_L, Z_s - Z_L). \tag{3}$$

Then, the laser spot $P(X_p, Y_p, Z_p)$ is determined as the intersection of Eqs. (1) and (2):

$$X_p = \frac{B_Y X_L - B_X Y_L}{B_Y x_p - B_X y_p} x_p,$$

$$Y_p = \frac{B_Y X_L - B_X Y_L}{B_Y x_p - B_X y_p} y_p,$$

$$Z_p = \frac{B_Y X_L - B_X Y_L}{B_Y x_p - B_X y_p} f. \tag{4}$$

So far, we have used $p(x_p, y_p, f)$ as the 3-D position of the laser spot on the image plane. It is not easy, however, to measure a point using physical length units on a digital image plane, while it is easy to measure it using pixel units. Even in such a case, we can determine the 3-D coordinates using pixel units instead of physical length units in a way as follows. First, we measure the distance of an arbitrary object and observe it with the endoscope. Suppose the position of the object is (X_t, Y_t, Z_t), and the displacement is t_t pixels in the x axis, and j_t pixels in the y axis. Suppose also the physical length of the pixel intervals is d_x in the x axis and d_y in the y axis. Then, the 3-D coordinates of the object can be represented as $(i_t d_x, j_t d_y, f)$, and the following equation is obtained:

$$\frac{X_t}{i_t d_x} = \frac{Y_t}{j_t d_y} = \frac{Z_t}{f}. \tag{5}$$

The 2-D coordinates of the laser spots (x_p, y_p) in Eq. (4) can be represented as

$$x_p = i_p d_x, \quad y_p = j_p d_y, \tag{6}$$

where i_p and j_p represent the position of the laser beam spots on the image plane when they are measured using pixel units in the x and y axis, respectively.

Then the 3-D coordinates (X_p, Y_p, Z_p) can be determined from Eq. (4) using Eqs. (5) and (6):

$$X_p = \frac{B_Y X_L - B_X Y_L}{B_Y i_p j_t X_t - B_X j_p i_t Y_t} i_p j_t X_t,$$

$$Y_p = \frac{B_Y X_L - B_X Y_L}{B_Y i_p j_t X_t - B_X j_p i_t Y_t} j_p i_t Y_t,$$

$$Z_p = \frac{B_Y X_L - B_X Y_L}{B_Y i_p j_t X_t - B_X j_p i_t Y_t} i_t j_t Z_t. \tag{7}$$

The parameters x_p, y_p, and f in Eq. (4), which should be measured in physical length units, disappear from Eq. (7), and the 3-D coordinates (X_p, Y_p, Z_p) can be expressed only by those parameters that can be measured in normal situations.

2.5 *Display of Rulers*

Once the 3-D position of the laser spot is measured by the previous method, we can estimate the size of objects near the spot. The system can display rulers virtually on the plane parallel to the image plane, and whose center is at the laser spot (Fig. 5). To depict the divisions of the scale according to its 3-D position, we should calculate the length of the interval of those divisions. Let u be the physical length of the interval, and u is set to 0.5 mm in the following examples. Then, we should calculate the length in pixels on the image plane that corresponds to u.

The length of a line segment on the plane $z=Z_p$ that passes the laser spot and is parallel to the image plane is reduced by the ratio of f/Z_p. The proper interval of the scale divisions is uf/Z_p. Even if the focal length f is unknown, the interval of the divisions can be determined from

$$\frac{f}{Z_p} = \frac{x_p}{X_p} = \frac{y_p}{Y_p} = \left(\frac{x_p^2 + y_p^2}{X_p^2 + Y_p^2} \right)^{1/2}, \tag{8}$$

by the ratio of the distance of the laser spot on the image plane $\sqrt{x_p^2 + y_p^2}$ to the distance of the laser spot from the optical axis $\sqrt{X_p^2 + Y_p^2}$.

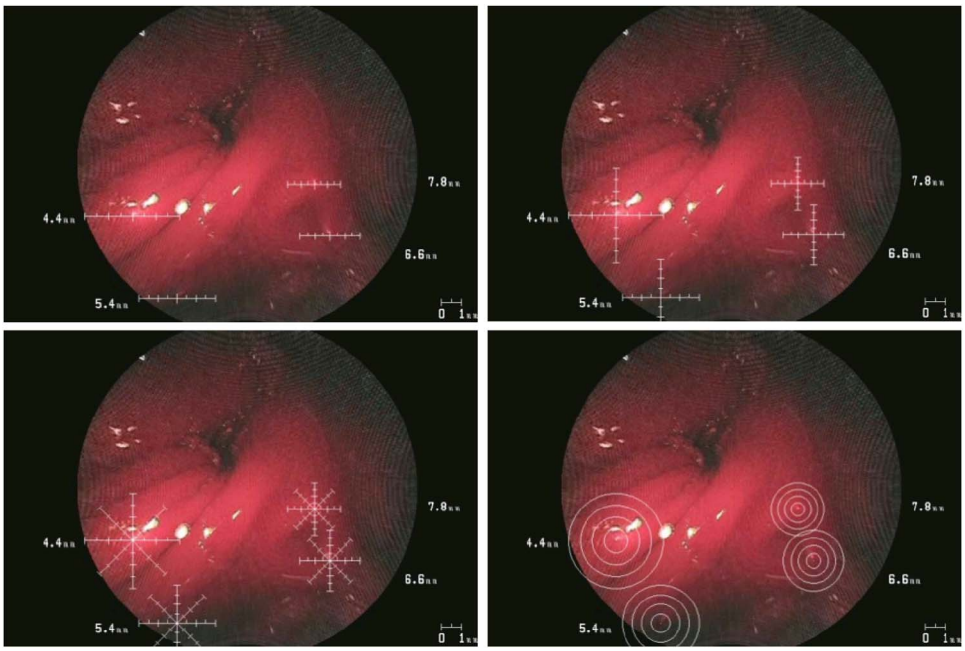

Video 1 Virtual rulers on laser spots (MPEG, 5.16 MB). [URL: http://dx.doi.org/10.1117/1.2800758.1]

In the same way, if the physical length on the image plane is unknown, the intervals of the divisions can be represented in pixels. In this case, the reduction ratio changes by the direction of the ruler to display. Suppose we should display it in the direction of θ in the real space. The interval of the divisions should be $uf \cos\theta / Z_p d_x$ pixels in the x direction and be $uf \sin\theta / Z_p d_y$ pixels in the y direction. Even if f/d_x or f/d_y is unknown, we only have to display the divisions by the ratio of the number of pixels to the laser spot on the image to the number of pixels to the spot from the lens optical axis.

In Video 1, four laser beams are projected on the gastric wall of a rat, and the distances to the four spots are measured. Four rulers are also displayed with those divisions whose intervals are calculated according to their distances. The rulers can be displayed in one, two, or four directions, or can be concentric circles.

2.6 *Rulers in-between the Laser Beam Spots*

When the system places a ruler parallel to the image plane, it marks the divisions repeatedly only with the same interval, since all the divisions of the scale should be equally placed both in the real space and on the image plane. However, a ruler that connects two laser spots is not always parallel to the image plane (Fig. 6). Though the divisions are equally placed in the real space, it does not hold for the virtual rulers on the image plane. We have to calculate all the positions of each division.

Suppose that we mark the divisions M_k $(k=0,1,2,\ldots)$ with the interval of u, starting at a laser spot $P_s(X_s,Y_s,Z_s)$ and ending at another laser spot $P_e(X_e,Y_e,Z_e)$. Then, (X_k,Y_k,Z_k), the 3-D position of the k'th division M_k can be calculated as:

$$X_k = \frac{(\|P_e - P_s\| - ku)X_s + kuX_e}{\|P_e - P_s\|},$$

$$Y_k = \frac{(\|P_e - P_s\| - ku)Y_s + kuY_e}{\|P_e - P_s\|},$$

$$Z_k = \frac{(\|P_e - P_s\| - ku)Z_s + kuZ_e}{\|P_e - P_s\|}, \tag{9}$$

where $\|P_e - P_s\|$ represents the distance between two laser spots and can be calculated by the method mentioned in Sec. 2.4. Thus, their corresponding positions on the image plane $m_k(x_k,y_k,z_k)$ can be calculated from (X_k,Y_k,Z_k) as:

$$x_k = \frac{X_k}{Z_k} f,$$

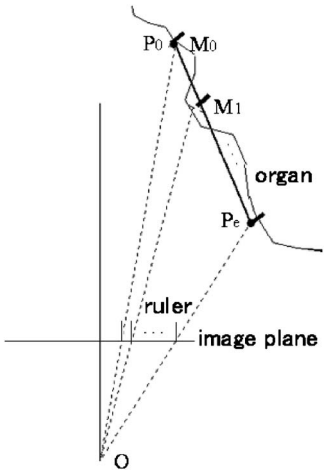

Fig. 6 Oblique ruler between laser spots.

$$y_k = \frac{Y_k}{Z_k} f,$$

$$z_k = f. \tag{10}$$

That means the k'th division of the scale should be marked at

$$\left(\frac{X_k}{Z_k} f, \frac{Y_k}{Z_k} f \right), \tag{11}$$

on the image.

In Eq. (10), the physical length is used in determining the positions of the divisions of the scale. We can also determine those positions if we have to use pixels as the unit. By observing an object with known displacement, as mentioned before, Eq. (5) gives

$$\frac{f}{d_x} = \frac{i_t Z_t}{X_t},$$

$$\frac{f}{d_y} = \frac{j_t Z_t}{Y_t}. \tag{12}$$

That means, from the 3-D coordinates (X_t, Y_t, Z_t) and their projection on the image plane (i_t, j_t) in pixels, we can determine the values f/d_x and f/d_y. Thus, Eq. (11), i.e., the position of the k'th division on the image plane, can be represented in pixels as (i_k, j_k) using d_x and d_y, the physical length per pixel in the x and y directions, respectively:

$$i_k = \frac{X_k f}{Z_k d_x} = \frac{X_k i_t Z_t}{Z_k X_t},$$

$$j_k = \frac{Y_k f}{Z_k d_y} = \frac{Y_k j_t Z_t}{Z_k Y_t}. \tag{13}$$

Therefore, we only have to mark the k'th division at

$$\left(\frac{X_k i_t Z_t}{Z_k X_t}, \frac{Y_k j_t Z_t}{Z_k Y_t} \right),$$

in pixels.

Thus we can depict oblique rulers between the spots. Figure 7 shows an example of displaying the rulers in-between the four laser spots.

3 Experiments

We have modified a commercially available endoscope Fujinon EC-450WM5, which is used for the lower gastrointestinal (GI) tract, with a 140-deg view field and 12.8-mm distal end diameter. The diameter of the optical fibers, via which the four laser beams are directed, is 120 μm. The maximum power of the laser beam is 6 mW, and the wavelength is set to 635 nm to lessen the beam absorption into tissues.

To evaluate the practicability, we used the proposed system to observe the gastric wall of a rat. The figures shown in Sec. 2 were taken during one of those experiments. To estimate the detection rate of the laser spot, we checked 1000 consecutive

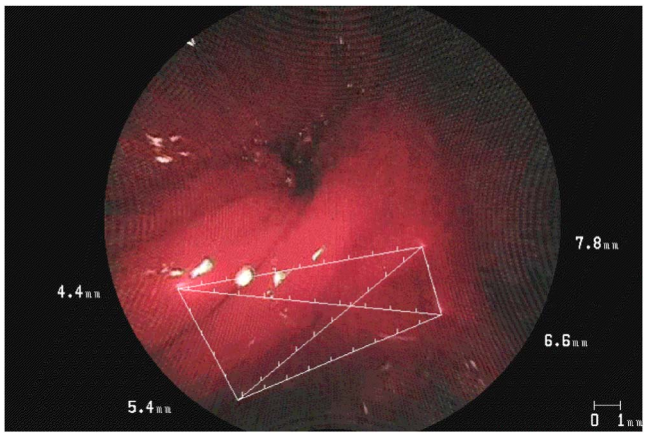

Fig. 7 Rulers between laser spots.

frames and found that the rate of correct detection was 85%. Most failures occurred when the system mistook reflection highlights for laser spots. It does not matter, however, when it comes to clinical applications, because physicians do not take the trouble to see highlighted areas to observe all the spot locations in each and every frame, but they only need their locations of interest. In addition, our system is made interactive, so that physicians press the foot switch only when they need 3-D measurements while seeing the motion of the laser spots. The detection rate increases to 97% for those areas without highlights.

The processing time for each frame with an Intel Xeon 5160, 3.00 GHz × 2 is as follows: 9.6×10^{-3} sec for the distortion correction, 6.3×10^{-3} sec for the laser spot detection, and 1.0×10^{-6} sec for the 3-D coordinate calculation and ruler display. Thus, the total processing time for a frame is 1.6×10^{-2} sec, so that all the procedures can be performed in real time.

To estimate the accuracy of the distance measurements, we observed a screen at a distance varying between 5 and 40 mm. We used the parameters obtained at 20 mm to measure the other distances in such a way as mentioned in Sec. 2.4, and found the differences between the distances that the system calculated and the actual ones are within the range of 0.2 mm. We also estimated the accuracy of the virtual rulers by observing graph paper at a distance varying between 5 and 40 mm. We compared the actual lengths on the graph paper and the lengths measured with the virtual ruler, and found that the average error in the measurement is 5.1%.

4 Conclusions

We present a laser beam endoscope system for 3-D measurements in real time. The system detects the laser spots automatically and calculates their 3-D coordinates by the triangulation method. Physicians can see the rulers that fit the 3-D position, and can measure the size and position of objects on undistorted images, similar to placing rulers on the surface of an organ.

Though we cannot use the proposed system for bedside diagnosis because it needs official medical device evaluation, the experiments using rats show the effectiveness of the system for clinical use.

References

1. R. B. Northrop, *Noninvasive Instrumentation and Measurement in Medical Diagnosis*, CRC Press, Boca Raton, FL (2002).
2. A. Katzir, *Lasers and Optical Fibers in Medicine*, Academic Press, San Diego, CA (1993).
3. B. J. Wood and P. Razavi, "Virtual endoscopy: a promising new technology," *Am. Fam. Physician* **66**(1), 107–112 (2002).
4. A. del Rio, D. Bartz, R. Jäger, Ö. Gürvit, and D. Freudenstein, "Efficient stereoscopic rendering in virtual endoscopy applications," *Proc. WSCG*, pp. 95–101 (2003).
5. F. Devernay, F. Mourgues, and È. Coste-Manière, "Towards endoscopic augmented reality for robotically assisted minimally invasive cardiac surgery," *Proc. Intl. Workshop Med. Imag. Augmented Reality IEEE*, pp. 16–20 (2001).
6. T. Thormählen, H. Broszio, and P. N. Meier, "Three-dimensional endoscopy," in *Medical Imaging in Gastroenterology and Hepatology*, F. Hagenüller, M. P. Manns, H. G. Musmann, and J. F. Riemann, Eds., Kluwer Academic Publishers, New York (2002).
7. D. Yelin, I. Rizvi, W. M. White, J. T. Motz, T. Hasan, B. E. Bouma, and G. J. Tearney, "Three-dimensional miniature endoscopy," *Nature (London)* **443**(19), 765 (2006).
8. M. Yamaguchi, Y. Okazaki, H. Yanai, and T. Takemoto, "Three-dimensional determination of gastric ulcer size with laser endoscopy," *Endoscopy* **20**(5), 263–266 (1988).
9. K. Hasegawa and Y. Sato, "Endoscope system for high-speed 3D measurement," *Syst. Comput. Japan* **32**(8), 30–39 (2001).
10. R. O. Duda, P. E. Hart, and D. G. Stork, *Pattern Classification*, 2nd ed., John Wiley and Sons, New York (2001).